Science of Remote Sensing 1 (2020) 100002

Contents lists available at ScienceDirect

Science of Remote Sensing

journal homepage: www.journals.elsevier.com/science-of-remote-sensing

The Global Ecosystem Dynamics Investigation: High-resolution laser ranging of the Earth's forests and topography

Ralph Dubayah [a,*], James Bryan Blair [b], Scott Goetz [c], Lola Fatoyinbo [b], Matthew Hansen [a], Sean Healey [d], Michelle Hofton [a], George Hurtt [a], James Kellner [e], Scott Luthcke [b], John Armston [a], Hao Tang [a], Laura Duncanson [a], Steven Hancock [a,f], Patrick Jantz [c], Suzanne Marselis [a], Paul L. Patterson [d], Wenlu Qi [a], Carlos Silva [a]

[a] Department of Geographical Sciences, University of Maryland, College Park, MD, USA
[b] NASA Goddard Space Flight Center, Greenbelt, MD, USA
[c] Northern Arizona University, Flagstaff, AZ, USA
[d] United States Forest Service, USA
[e] Brown University, Providence, RI, USA
[f] The University of Edinburgh, Edinburgh, United Kingdom

ARTICLE INFO

Keywords:
Lidar
Ecosystem structure
GEDI
Biomass

ABSTRACT

Obtaining accurate and widespread measurements of the vertical structure of the Earth's forests has been a long-sought goal for the ecological community. Such observations are critical for accurately assessing the existing biomass of forests, and how changes in this biomass caused by human activities or variations in climate may impact atmospheric CO_2 concentrations. Additionally, the three-dimensional structure of forests is a key component of habitat quality and biodiversity at local to regional scales. The Global Ecosystem Dynamics Investigation (GEDI) was launched to the International Space Station in late 2018 to provide high-quality measurements of forest vertical structure in temperate and tropical forests between 51.6° N & S latitude. The GEDI instrument is a geodetic-class laser altimeter/waveform lidar comprised of 3 lasers that produce 8 transects of structural information. Over its two-year nominal lifetime GEDI is anticipated to provide over 10 billion waveforms at a footprint resolution of 25 m. These data will be used to derive a variety of footprint and gridded products, including canopy height, canopy foliar profiles, Leaf Area Index (LAI), sub-canopy topography and biomass. Additionally, data from GEDI are used to demonstrate the efficacy of its measurements for prognostic ecosystem modeling, habit and biodiversity studies, and for fusion using radar and other remote sensing instruments. GEDI science and technology are unique: no other space-based mission has been created that is specifically optimized for retrieving vegetation vertical structure. As such, GEDI promises to advance our understanding of the importance of canopy vertical variations within an ecological paradigm based on structure, composition and function.

1. Introduction

For over 50 years NASA, along with other international space agencies, has supported important scientific and policy issues related to the present and future states of the Earth's carbon and water cycles, its climate, its habitat suitability, and other ecosystem services using a constellation of Earth orbiting satellites. The three-dimensional structure of forests and their above-ground carbon content (as estimated from above-ground biomass density, hereafter AGBD) continue to be the most crucial information gaps in the observational archive. The most direct and accurate way of obtaining this detailed vertical structure at the resolution and accuracy required is through lidar remote sensing. While airborne lidar remote sensing of the land surface continues to accelerate, there have been only a few non-atmospheric spaceborne lidars, beginning with the Shuttle Laser Altimeter (SLA) (Garvin et al., 1998), which was followed by the ICESat (Schutz et al., 2005) and the current ICESat2 missions (Abdalati et al., 2010). ICESat stopped data collection in 2009. These missions, along with the continued development and application of analogue spaceborne data from NASA's large-footprint airborne instrument LVIS (the Land Ice and Vegetation Sensor) (Blair et al., 1999)

* Corresponding author. 1149 Lefrak Hall, 7251 Preinkert Dr, College Park, MD, 20742, USA.
E-mail address: dubayah@umd.edu (R. Dubayah).

https://doi.org/10.1016/j.srs.2020.100002
Received 10 September 2019; Received in revised form 5 January 2020; Accepted 7 January 2020
Available online 22 January 2020

have demonstrated the potential value of waveform lidar observations of canopy structure from space.

To fill this ongoing gap in widespread observations of forest canopy structure, the Global Ecosystem Dynamics Investigation (GEDI) was proposed and selected as part of NASA's Earth System Science Pathfinder (ESSP) Earth Ventures 2 (EV-2) competition. GEDI was successfully launched from Cape Canaveral, Florida in the Dragon capsule of SpaceX CRS-16 on board a Falcon 9 rocket and subsequently installed in its new home on the Japanese Experiment Module-Exposed Facility (JEM-EF) on board the International Space Station (ISS) in December of 2018.

GEDI will sample about 4% of the Earth's land surface over its two-year nominal mission, acquiring over 10 billion cloud-free shots. GEDI lidar observations are used to create data sets on canopy height, canopy cover and vertical profile, canopy leaf area index and profile, topography, and footprint-level and gridded AGBD, among others. These are the first spaceborne measurements from an instrument specifically optimized to measure vegetation structure and which form the basis of critical reference data sets. GEDI data are anticipated to be used by the scientific community for far ranging applications, by themselves, and in fusion with other existing and planned radar missions, such as TerraSAR-X add-on for Digital Elevation Measurement (TanDEM-X) (Krieger et al., 2007), NASA-ISRO SAR Mission (NISAR) (Rosen et al., 2015), Sentinel-1 (Torres et al., 2012) and BIOMASS (Le Toan et al., 2011), along with other optical data sets such as from Landsat and MODIS.

Here we provide an overview of the GEDI mission. We first discuss its scientific goals and objectives and explain its rationale within a context of the scientific importance of ecosystem structure for the main application areas of GEDI: land surface carbon balance and biodiversity. We next provide an outline of GEDI mission implementation, including its science and measurement requirements and describe how GEDI measurements are used to produce its science products and their associated algorithms. We then turn our focus to the key technical elements of the lidar instrument, including its specifications and measurement capabilities. Lastly, we summarize the GEDI approach to calibration and validation, both pre- and post-launch.

2. Science objectives and rationale

GEDI's overall goal is to help advance our ability to characterize the effects of changing climate and land-use on ecosystem structure and dynamics. GEDI seeks to address three core science questions related to this goal:

1. What is the above-ground carbon balance of the Earth's tropical and temperate forests?
2. What role will the land surface play in mitigating atmospheric CO_2 in the coming decades?
3. How does ecosystem structure affect habitat quality and biodiversity?

Trends in climatic change and non-sustainable land-use are dramatically affecting the Earth's environment (National Research Council, 2007). Quantifying land cover structure and dynamics is a prerequisite for understanding and managing these challenges, and it is the horizontal and vertical structure of ecosystems that are critically needed, especially with regards to potential carbon emissions to the atmosphere from the land surface (Dubayah et al., 2010).

Although fossil fuels contribute the majority of human emissions (9.9 $\pm$ 0.5 Petagrams Carbon per Year, or PgC/yr, in 2017), the release of vegetation carbon from deforestation is the second largest source term driving warming (1.4 $\pm$ 0.7 PgC/yr) (IPCC et al., 2007; Quéré et al., 2018). (Note: here we intend "deforestation" to refer to disturbances that lead to a loss of forests, such as logging and fire. Our use of "regrowth" refers to areas which have been deforested but return to a forested state. We include degradation, that is the incomplete loss of canopy cover, in the above, but the ability of GEDI to detect degradation is still to be determined). Global flux analyses suggest terrestrial ecosystems must be absorbing roughly 3.8 $\pm$ 0.8 PgC/yr (Quéré et al., 2018), more than one-third of the fossil carbon emitted per year. However, the location of vegetation carbon sources and sinks are poorly known from either existing inventory data or the remote sensing record but may have large effects on climate forcings.

Relative to other terms in the carbon balance, the uncertainties resulting from deforestation and subsequent regrowth are large because we do not know the true magnitude of global forest biomass stocks as they exist today. Improving knowledge of biomass stocks in tropical biomes is particularly urgent because of the potential benefits from reducing deforestation emissions. While area of deforestation can be mapped using optical remote sensing (Hansen et al., 2010, 2013), lack of information on forest AGBD limits the precision of measuring deforestation emissions (Houghton, 2003, 2013; Houghton et al., 2009). The limitations in current large-scale biomass estimation and error analysis have led to diverging estimates that must often be reconciled (Mitchard et al., 2013). Attempts to estimate carbon emissions resulting from pan-tropical deforestation using ICESat lidar observations and land cover data achieve different results (e.g. see (Saatchi et al., 2011; Baccini et al., 2012; Harris et al., 2012; Tyukavina et al., 2015)). A major limitation and source of uncertainty is the sparseness of the lidar observations themselves, which prohibits accurate biomass estimation at fine scales (<10 km) (Houghton et al., 2010). For example, the pantropical maps of Saatchi et al. (2011) and Baccini et al. (2012) were based on about 5 million and 3 million ICESat shots, respectively. In contrast, after its first 3 months on-orbit, GEDI has accumulated almost 200 million observations over the pantropical land areas.

Quantifying the future state of forests in the coming decades, that is the carbon sequestration trajectory of existing forests and reforestation and afforestation, is imperative for managing forests in the context of climate change mitigation (IPCC et al., 2007; Pan et al., 2011). An integrated modeling capacity is required for evaluating the role the land surface plays in alternative climate mitigation and adaptation strategies and accurately projecting carbon and biological resources in a changing world intimately linked to human activities. Much progress has made over the last decade integrating prognostic ecosystem models, such as the Ecosystem Demography (ED) model and FORMIND, with canopy height and structure derived from lidar at both local and regional scales (Hurtt et al., 2004, 2010, 2016, 2019; Thomas et al., 2008; Knapp et al., 2018). The great advantage of such initialization is that it provides the carbon status and successional trajectory of the forest as it actually exists today, rather than what it might be under some potential vegetation state. This then enables the modeling of realistic stocks and fluxes under climate change and land use change scenarios. What is needed are accurate and wide-spread ecosystem structure data to enable high spatial resolution modeling.

Lastly, ecosystem structure is increasingly seen as an important determinant of habitat quality, and therefore suitability, as well as a factor in species distribution, richness and abundance (Pereira et al., 2013). The status of forest biological diversity at regional and global scales is poorly known due to a paucity of canopy structural measurements required for quantifying habitat (Mace et al., 2005; Secretariat of the Conven, 2010; De Vos et al., 2015; Pimm and Raven, 2000; Pimm et al., 2014; Bergen et al., 2009). At the same time, observational requirements for vegetation 3D structure measurements from space using lidar for biodiversity and habitat assessments are well established (Bergen et al., 2009; Turner et al., 2003). Such structure is also a key element of strategies that jointly optimize forest carbon preservation and atmospheric sequestration while protecting and expanding habitat, say through forest restoration to create corridors that connect forest reserves (Brancalion et al., 2019; Jantz et al., 2014).

3. GEDI mission implementation overview and science requirements

In this section we provide an overview of GEDI mission definition and

implementation. This includes the articulation of science requirements, observational objectives, and methodological approaches towards the creation of data sets required to fulfill its science objectives and address its science questions.

3.1. Mission implementation

The GEDI instrument is housed on the JEM-EF (Fig. 1). GEDI measurements are made day and night and are taken continuously over the Earth's land surfaces between 51.6° N & S latitude, covering the tropical and temperate forests of the Earth. As with all optical remote sensing, lidar observation cannot be made through dense cloud cover.

The instrument uses an active across-track pointing system to help eliminate coverage gaps that result from ISS orbital variations. These occur because the ISS is not maintained in a repeating orbit and can get "stuck" in orbital resonances that essentially repeat orbital tracks and result in large coverage gaps (Fig. 2). GEDI's pointing capability also allows it to target specific plot locations or other areas of interest to within about 35 m. Over the 2-year mission, GEDI attempts to distribute laser tracks methodically and as evenly spaced as possible around the Earth, following a set of prescribed Reference Ground Tracks (RGTs) that maximize sampling.

GEDI uses an advanced laser remote sensing system whose sole observable is the returned lidar waveform (Fig. 3). From this waveform a variety of canopy and waveform metrics may be derived such as canopy height, canopy vertical profile and Relative Height (RH) energy metrics (Tang et al., 2012; Drake et al., 2002) as well topographic surface elevation.

The system is comprised of 3 lasers, one of which is split into two beams ("coverage" beams), while the other two remain at full power ("power" beams). Each laser fires 242 times per second. At any one time, 4 beams, each with footprint diameter of ~25 m, are incident on the ground. Each of these 4 beams is then dithered every other shot across track, to produce 8 tracks of data, separated by about 600 m across the flight track direction within a ~4.2 km swath. For any one track, footprint centers are separated by 60 m along track (or equivalently, 35 m from one edge to the next) because every other shot from a laser beam is dithered (Fig. 4).

The nominal mission length is two years after its on-orbit checkout (April 2019). Data are always collected over the land surface, but the lasers are ramped down over ocean passes to conserve lifetime, collecting only enough ocean data to permit precision orbit determination which underpins the accuracy of final geolocation. GEDI uses its own Global Positioning System (GPS), Inertial Measurement Unit (IMU), and information from three star trackers that permit GEDI to georeference each laser pulse to within 10 m (1 σ) (i.e. assuming a distribution of geolocation errors whose mean is zero, and whose standard deviation is 10 m) on the Earth's surface.

The GEDI Science Team (GST) is responsible for delivery of all data sets to the Land Process (LP) and Oak Ridge National Laboratory (ORNL) Data Archive and Analysis Centers (DAACs) with specified delivery times and latencies (Table 1).

3.2. Level 1 science requirements

During its development, GEDI was guided by a process that linked its science objectives to "Level 1" science requirements (L1). GEDI data products must demonstrate that they are sufficient to meet these requirements. The data products themselves, in turn, determine a tightly coupled cascade of linked mission operations requirements, measurement and instrument requirements, along with the definition of the types of measurements, their characteristics, their required precision and accuracy, and projected instrument performance.

GEDI has two L1 science requirements that define mission success. Measurement and mission requirements all trace back towards achieving these two requirements:

L1A: Acquire lidar canopy vertical profile data required to estimate AGBD for the Earth's global tropical and temperate forests at $\leq$ 1 km resolution. At the end of a two-year mission, AGBD of at least 80% of the 1 km cells shall be estimated with a precision (standard error) of the larger of ±20 MgC/ha or 20% of the estimate.
L1B: Acquire uniformly distributed transects of tropical & temperate forest canopy vertical profiles from the top of canopy to the ground in conditions of 95%–98% canopy cover, respectively for the coverage and full power beams. Profiles shall have 25 m spatial resolution, with 1 m vertical resolution and along track spacing of footprints <60 m.

These requirements were created to reflect two objectives: (1) provide data sets that enable the meeting of the GEDI science objectives, and (2) fully constrain the engineering and mission implementation designs such that these data sets may be created. The ecosystem science community has noted that accurate AGBD maps are needed at scales from 100 m–1 km, and that estimates of AGBD at these scales should meet a precision of about 20% (Hall et al., 2011). A 1 km map of biomass, whose vast majority of grid cells meet this precision of the mean, would represent a significant advance forward and provide the most accurate baseline map of carbon stocks to date. The constraint of 80% cells meeting such a precision requirement reflects the reality of scientific, environmental, and mission constraints that may limit achieving such accuracies for every single 1 km cell. For example, persistent cloud cover, or random orbital permutations may limit coverage in an area. Likewise,

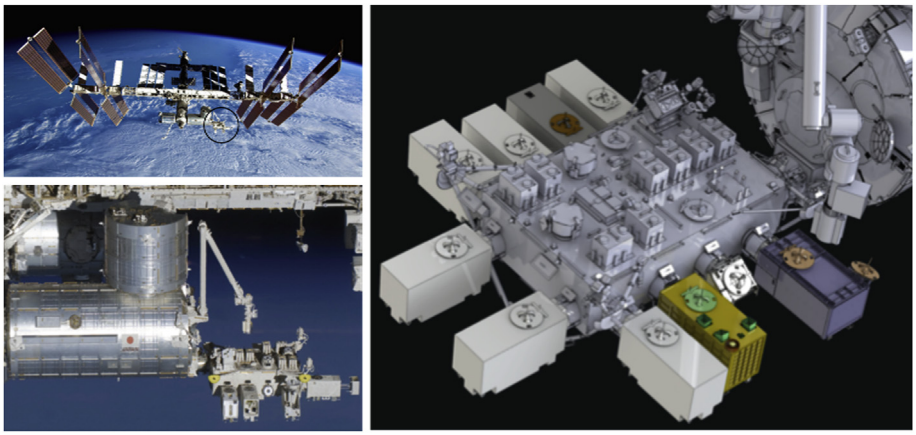

Fig. 1. GEDI is located on the Japanese Experiment Module (bottom left) of the International Space Station (top left) and attached to the Exposed Facility of this module (bottom, GEDI shown highlighted).

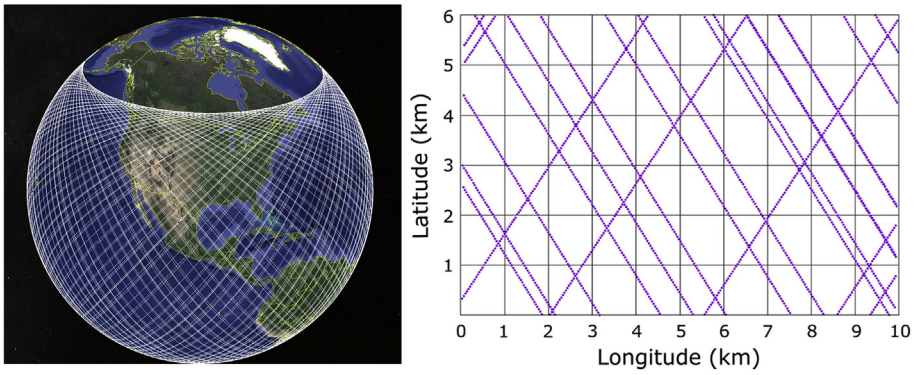

Fig. 2. Two weeks of GEDI orbital tracks (left). Each line represents one track (around which the 8 laser tracks are arranged). (right) Simulated spatial configuration of GEDI tracks after a two-year nominal mission length at the equator. Note the irregular pattern of tracks which results from the ISS precessing orbit. The GEDI PCS is used to fill-in between some of the large gaps to provide more even coverage. Coverage is worst at the equator and 50% of the tracks have been removed to simulate the impacts of clouds.

calibration equations that translate GEDI waveforms into estimates of ABGD cannot be fully optimized by grid cell, rather they are optimized by plant functional type (PFT) and region. Therefore, residual errors on any particular cell may limit accuracy for that cell. Our experience during mission development was that achieving a rate significantly beyond 80% would have required a longer time on orbit to eliminate coverage gaps, which in turn would require lasers that were capable of operating longer without significant degradation, as well as certifying that other instrument systems all could operate longer in the space environment. The combination of these would have made mission implementation impossible within the funding constraints. The long term performance of the lasers is discussed in detail in Stysley et al. (2015).

4. GEDI data products and algorithms

Lidar waveforms quantify the vertical distribution of vegetation by recording the amount of laser energy reflected by plant material (stems, branches, and leaves) at different heights above the ground. From GEDI waveforms, four types of structure information can be extracted: surface topography, canopy height metrics, canopy cover metrics, and vertical structure metrics. Signal processing is used to identify the ground within the waveform. The distribution of laser energy above the ground can be used to determine the height and density of objects (stems, leaves and branches) within the footprint. The view geometry and active use of light by lidar allows the ground to be identified through small gaps in the tree canopy, enabling unsaturated measurements of much denser forests than is possible with either passive optical or short wavelength radar systems.

4.1. Data levels

GEDI science data products include footprint and gridded data sets that describe the 3D features of the Earth. These data products are assigned different levels (Table 1), which indicate the amount of processing that the data has undergone after collection. Note that the term "Level 1" as applied to science requirements is not related to the "level" label of the data products.

4.1.1. Level 1: raw and geolocated waveforms

The raw GEDI waveforms as collected by the GEDI system are denoted as L1A. These waveforms are geolocated and positioned properly relative to the Earth's ellipsoid after orbital and pointing analyses based on information from GEDI's GPS and star trackers and stored as L1B data. L1B are not yet processed to identify the ground or canopy height.

4.1.2. Level 2: footprint level canopy height and profile metrics

The waveforms are processed to identify ground elevation, canopy top height, and the relative height (RH metrics) in the L2A data set. In L2B, various canopy metrics are calculated, including canopy cover fraction, total leaf area index (LAI), and the vertical foliage profile, that is, how LAI varies with height from the top of the canopy to the identified ground.

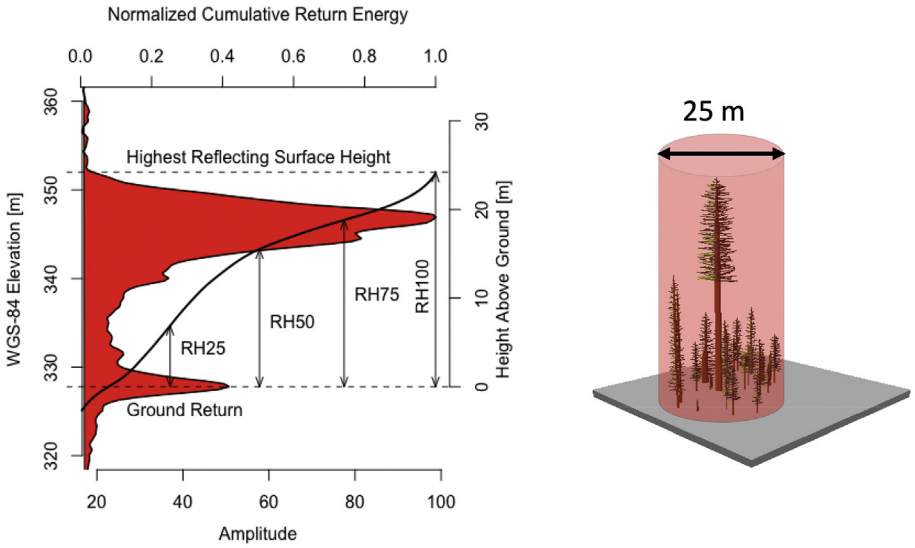

Fig. 3. GEDI waveform. A near-infrared pulse of laser energy is fired towards the surface where it is reflected by leaves and branches within a nominal 25 m diameter footprint (shown at right). The returned waveform (shown on left) is processed to find ground topography, canopy height, and various relative height (RH) metrics. From these metrics a variety of other products may be derived, including leaf density profile, canopy cover and aboveground biomass.

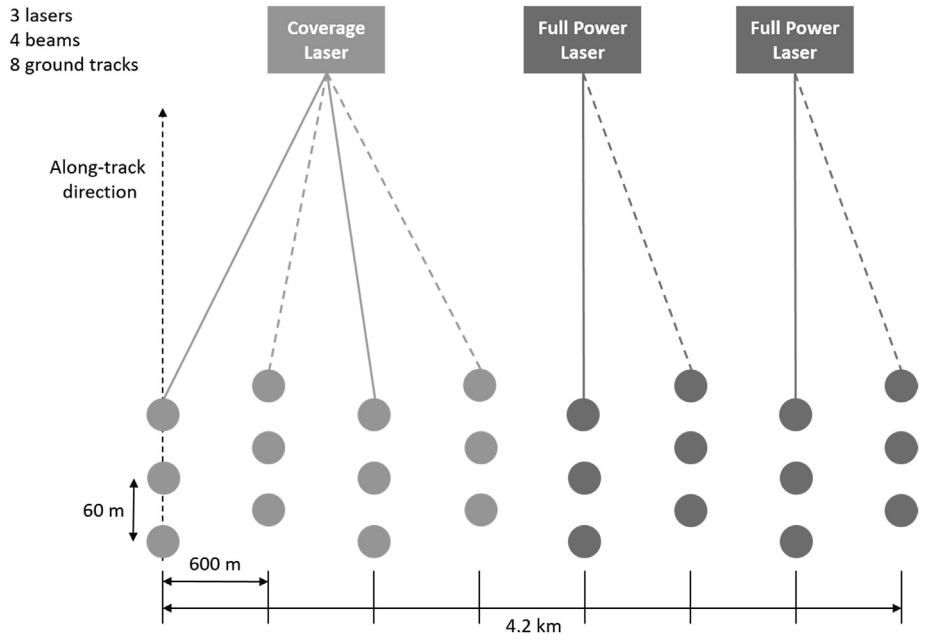

Fig. 4. GEDI beam pattern. Note that the along-track and across-track distances are not to scale (across track distance is about 10x larger). At any one instant, four laser pulses from the 3 lasers hit the ground. These are then dithered across-track to produce a complement of 8 tracks, with a gap of one shot along-track.

Table 1
GEDI data products. MOC = Mission Operations Center. IOC=Initial On-orbit Checkout.

Product/ Data file	Description	First Data Delivery After IOC	Data Latency	Archive Site
GEDI00_B[a]	Level 0B Instrument Products	Within 24 h of receipt at MOC	Within 24 h of receipt at MOC	LPDAAC
GEDI01_A[a] GEDI01_B	Level 1B Geolocated Waveforms and Fitted Parameters	First 2 months of L1B released at 6 months	4 months in monthly intervals	LPDAAC
GEDI02_A	Level 2A Footprint Elevation and Height Metrics	First 2 months of L2 released at 6 months	4 months in monthly intervals	LPDAAC
GEDI02_B	Level 2B Footprint Cover and Vertical Profile Metrics	First 2 months of L2 released at 6 months	4 months in monthly intervals	LPDAAC
GEDI03	Level 3A Gridded Land Surface Metrics	Populated with first 2 months of L2 data at 6 months	4 months in monthly intervals	ORNLDAAC
GEDI04_A	Level 4A Footprint Aboveground Biomass Density	First 12 months of data at 17 months	6 months after global sampling required to meet L1 requirement	ORNLDAAC
GEDI04_B	Level 4B Gridded Aboveground Biomass Density	First 12 months of data at 17 months	6 months after global sampling required to meet L1 requirement	ORNLDAAC

[a] Note: GEDI L0 and L1A data sets are not released to the public.

4.1.3. Level 3: gridded canopy height metrics and variability

Level 3 products are gridded by spatially interpolating L2 footprint estimates of topography, canopy height, canopy cover, canopy height, LAI, vertical foliage profile and their uncertainties.

4.1.4. Level 4: footprint and gridded aboveground biomass estimates

Level 4 products are the highest level of GEDI product, represent the output of models and require the most post-processing. Footprint metrics derived from the L2 data products are converted to footprint estimates of AGBD using calibration equations. Subsequently, these footprints are used to estimate mean AGBD and its standard error in cells of size 1 km × 1 km using statistical theory. The process of producing footprint (L4A) and gridded (L4B) AGBD estimates is described in more detail below.

4.2. Demonstrative products

GEDI data enable the derivation of other types of products, which are demonstrative for limited areas. The intention of these is to illustrate how methods developed as part of GEDI may be used to create these products, enabling downstream efforts for applying these to much larger, and even global areas. In particular, the data products associated with biomass change, ecosystem modeling, biodiversity and habitat are all demonstrative products and not produced over the entire extent of GEDI observations as part of its official mission. Nonetheless, we anticipate that such products will be made using GEDI data in the future.

4.2.1. Prognostic ecosystem modeling

GEDI height distributions are used to initialize the height-structured Ecosystem Demography model (ED) (Hurtt et al., 1998; Moorcroft et al., 2001). Once initialized, the ED model is capable of producing estimates of contemporary carbon stocks, carbon fluxes, and future carbon sequestration potential under alternative land use and climate change scenarios. Prior to GEDI, the model has been used extensively in a variety of biomes and applications with heights initialized from airborne lidar data (Hurtt et al., 2004, 2010, 2016, 2019; Thomas et al., 2008). The GEDI prognostic ecosystem modeling demonstrative products will apply the same model-data framework pioneered using airborne data to GEDI data over a significant region of the world to illustrate the potential for spaceborne lidar in large scale carbon model applications.

4.2.2. Enhanced height and biomass mapping using TanDEM-X

GEDI is a sampling mission and is therefore limited in the spatial resolution of the grids (wall-to-wall) that can be produced. One way to achieve finer, continuous spatial resolution is to combine these data with

other remote sensing data. GEDI, in collaboration with the German Aerospace Center (DLR) has focused on the use of the TanDEM-X data for enhanced height and biomass mapping. TanDEM-X is an X-band interferometric SAR capable of producing estimates of canopy height and structure using radiative transfer models. GEDI data are used to calibrate these models to produce estimates of height and biomass at much finer resolution than the 1 km grid GEDI produces by itself (Qi et al., 2019). Additionally, when used within our statistical framework, this approach allows for estimates where there are no GEDI data available, either because of clouds, or through normal sampling variation.

4.2.3. Biomass change using fusion with Landsat

Landsat data have been used to provide a global record of forest disturbance going back almost 30 years. GEDI data will intersect many of these deforestation patches and provide an estimate of present-day biomass. The biomass loss that occurred at the time of deforestation cannot be measured directly, but may be estimated through a time-for-space substitution approach such as that of Tyukavina et al. (2015) who employed lidar-derived biomass and Landsat forest disturbance maps to quantify pan-tropical aboveground carbon loss. GEDI biomass change will also include regrowth and associated carbon stock increase using disturbance history data. By examining forest loss and gain pixels in tropical and temperate forests, as identified by Tyukavina et al. (2015), an estimate of the net aboveground carbon balance between forest loss and subsequent regrowth may be calculated.

4.2.4. Biodiversity and habit model outputs

Climate, productivity, habitat composition, and habitat structure are primary determinants of animal distributions and habitat use (Huston, 1994; MacArthur and MacArthur, 1961; Whittaker et al., 2001). Three-dimensional habitat structure, in particular, has been the focus of recent interest since aircraft and spaceborne lidar have greatly improved our ability to test hypotheses relating species distributions relative to factors like vegetation height and canopy heterogeneity. Currently, many global conservation priorities are informed by coarse, expert drawn range maps (Pimm et al., 2014; IUCN, 2019). Using GEDI vegetation structure measurements, MODIS derived indicators of vegetation dynamics, species presence/absence observations, and databases of species traits, we are developing habitat distribution models (Burns et al., 2020) for threatened and endangered forest species which may significantly improve estimates of endangerment (Schnell et al., 2013). We expect integrating GEDI with a suite of other climate and remote sensing variables will improve assessments of conservation priorities.

4.3. Algorithm summaries

In this section we briefly summarize the algorithms used to generate each data product. The physical theories, mathematical procedures and model assumptions that are used in the creation of these data products are described in detail in the Algorithm Theoretical Basis Documents (ATBDs) https://gedi.umd.edu/data/documents/. These algorithms are implemented within the GEDI Science Data Processing Center to create the final data products.

4.3.1. Level 1

The Level 1 data includes Level 1A data, which are not publicly released, that contain the raw return waveform data along with detailed information on the transmitted and received waveform processing. The Level 1B data product contains the laser transmitted waveform, positioned laser received waveform and ancillary information as described next (Fig. 5). The first and last sample bins of the telemetered waveform record are precisely positioned (geolocated) within a geodetic reference frame defined by the International Terrestrial Reference Frame (ITRF) (Petit et al. 2010). The geolocated heights are relative to the WGS-84 ellipsoid. The geolocation is computed using the altimeter laser ranges to the first and last sample bins of the laser return waveform records, the data from GEDI's dual frequency GPS receiver for precise positioning, and a three-camera head star tracker system where each head contains a Micro-Electronics Measurement System (MEMS) with multi-axis gyros and accelerometers for the computation of the precise pointing of each laser beam. These 3 observations are combined using a variety of models, algorithms, and corrections to determine the laser waveform geolocation. These include the determination of the instrument position and laser pointing within a consistent geodetic reference frame, the correction for atmospheric refraction path delay, ranging and time-tag corrections, and geophysical corrections such as ocean and solid earth tides and geoid. Range is determined relative to the center of the laser transmit pulse, defined as the center of a gaussian distribution with baseline mean noise fit to the transmitted laser pulse.

At the time of publication, horizontal geolocation accuracy for calibrated final products is between 10 and 20 m and the vertical accuracy is on the order of 50 cm. These error statistics are indicative of early mission geolocation performance, with further improvements expected through post-processing and pointing, ranging and timing calibration updates. Note that the altimeter itself has 2 cm precision, and the geolocation height error is dominated by the positioning and pointing error. The post-launch calibration consists of an integrated residual analysis of the returned waveform ranging observations. For GEDI, altimeter range observations from ocean scans and "round"-the-world scans along with dynamic crossovers are used to calibrate and correct the systematic pointing and ranging errors in the form of biases, trends and orbital variation parameters (Luthcke et al., 2000, 2005). The calibration process is expected to reduce the geolocation error down to 8 m horizontal and 10 cm vertical.

4.3.2. Level 2

4.3.2.1. Level 2A. L2A processing uses the geolocated received waveform L1B product and computes footprint-level elevation and canopy heights. We compute canopy height by subtracting the elevation of the highest detected return from the elevation of the center of the lowest mode ("ground") in the received waveform (Hofton et al., 2000). These ranging points are identified during processing of the received waveform, and first and last sample bin geolocation in the L1B product are interpolated to geolocate the ranging points. The received waveform processing involves smoothing the signal to minimize noise, identification of signal and noise sections of the waveform, and locating the center of each mode between the highest and lowest detected returns in each waveform. The L2A product also includes the height above the ground of each energy quantile in the received waveform (relative height metrics as shown in Fig. 3) and are expressed as a height above the ground. An early, on-orbit example of L2A data is shown below (Fig. 6).

4.3.2.2. Level 2B. The L2B processing generates the footprint-level canopy cover and vertical profile metrics. We first compute vertical canopy energy distribution by subtracting the ground component from the received waveform. Next, we estimate the vertically resolved directional canopy gap probability of an individual footprint using the vertical canopy energy distribution and ground energy (Ni-Meister et al., 2001). The ratio of canopy to ground reflectance is also needed in the estimation process. Its value is extracted from a gridded ancillary dataset, which is initialized with constants over different biomes and will be updated in an iterative way as GEDI observations accumulate (Armston et al., 2013). Leaf Area Index (LAI) is calculated from the vertical distribution of canopy gap probability (Tang et al., 2012). We ignore variations in leaf angle distribution and clumping effects by assuming a random distribution of vegetation elements. Finally, we calculate foliage height diversity (FHD) using the generated vertical LAI profile at each footprint.

4.3.3. Level 3

The GEDI L3 gridded Land Surface Metrics are derived from L2

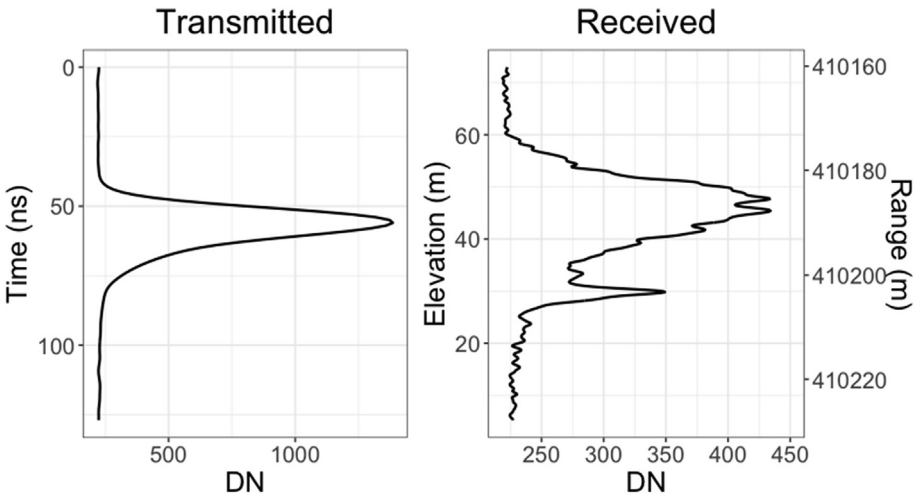

Fig. 5. Actual on-orbit laser transmitted (left) and corresponding received (right) waveforms from GEDI. The elevation relative to the WGS-84 ellipsoid and range from the center of the transmitted waveform to the received waveform sample bins are shown. Geolocated waveforms and ancillary parameters are given in the GEDI L1B data product.

footprint quantities by optimally interpolating to produce an average value for each cell of a 1 × 1 km grid. The footprint spot quantities are assumed to contain signal, having both a deterministic and zero-mean stochastic part, and an additive error that is uncorrelated with distance. The concept is to linearly combine these noisy data in a way such that the resulting signal interpolates are unbiased and have minimum mean-squared error. This interpolation is a function of the determined signal covariance, initially assumed to be varying only with distance, and is constructed locally for each grid cell from the footprint quantities themselves within a determined correlation length. Pre-launch testing has shown that both Ordinary and Universal Kriging are adequate since the domain over which the estimates are made is sufficiently small, and the covariance is determined locally for each grid cell using data from the grid cell and surrounding cells. For Ordinary Kriging, we assume the deterministic part is a stationary mean.

4.3.4. Level 4

4.3.4.1. Level 4A. The L4A footprint data product is aboveground biomass density (Mg · ha^{-1}) for individual GEDI footprints. Footprint AGBD is derived from linear models that relate GEDI L2 waveform height metrics to field-estimated aboveground biomass. The GEDI approach to footprint model selection is data driven. Candidate models are stratified by plant functional type and region, with natural-logarithm or square root transformations on the response and predictor variables. These transformations linearize the relationship between AGBD and waveform height metrics, ensure that predictions are non-negative, and stabilize the residual variance.

A challenge to developing globally representative models to predict AGBD using remote sensing is the relatively small number of locations available for algorithm training and testing. To overcome this problem, the GEDI calibrations are developed using a waveform simulator to

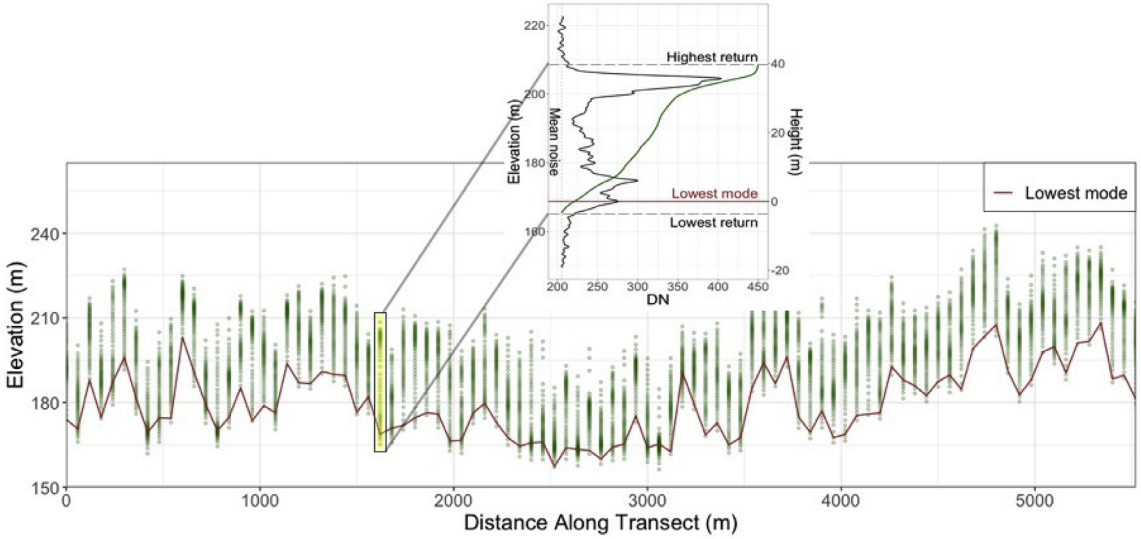

Fig. 6. GEDI data from one track acquired over Brazil processed to L2A. The L2A processing takes geolocated waveforms and identifies the highest and lowest returns and the center of each mode between these points, with the ground elevation corresponding to the elevation of the lowest mode. Each vertical green bar in the lower figure shows the position (elevation) of energy quantiles (0–100%) for a waveform along-track, where dark green indicates higher return energy (ground or more canopy material) and light green indicates lower return energy (less canopy material). The upper inset shows an example received waveform represented in lower figure, with locations of the highest return, lowest return (gray dashed lines), and center of the lowest mode (red line) indicated. (For interpretation of the references to colour in this figure legend, the reader is referred to the Web version of this article.)

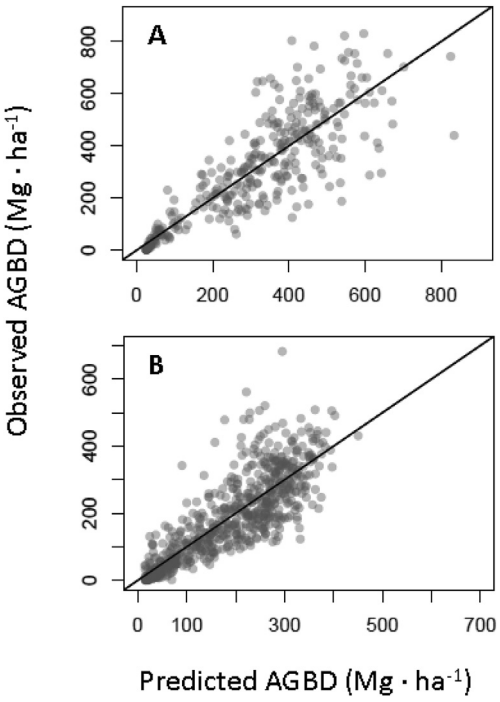

Fig. 7. Unbiased footprint-level relationships between predicted and observed AGBD in two combinations of PFT and region. The predictions are from generalized linear models developed using waveform relative height metrics. (A) Evergreen Broadleaf Trees in Australia; (B) Deciduous Broadleaf Trees in North America. The percentage RMSE is 30.7%, and 38.2%, respectively. Solid line is the one to one relationship.

produce simulated GEDI waveforms from discrete-return airborne lidar (Hancock et al., 2019). We produce thousands of training samples in temperate and tropical regions by associating height metrics from simulated waveforms with field-estimated AGBD. This extends previous efforts by developing algorithms that are representative of a wider range of ecosystem structural conditions than has previously been possible.

The GEDI footprint models represent four plant functional types and all continents except Antarctica (e.g. see Fig. 7). The plant functional types are deciduous broad-leaf trees, evergreen broad-leaf trees, evergreen and deciduous needle-leaf trees, and combinations of woodlands, grasslands and shrubs. The selection framework compares models with different predictor variables, stratifications, and transformations to identify models with the best performance that meet assumptions of the algorithms used to generate the L4B 1 km gridded AGBD data product (Patterson et al., 2019; Saarela et al., 2016; Ståhl et al., 2016).

A second challenge is ensuring that the GEDI models are transferrable outside the domain of calibration. Even though the calibration dataset contains simulated waveforms in more than 27 countries on six continents, important regions are under-represented, including the forests of continental Asia and Africa, and the evergreen broadleaf forests throughout the islands of Southeast Asia and north of Australia. To produce GEDI algorithms that are robust to this kind of uncertainty, we developed a cross-validation framework that explicitly evaluates model performance outside the geographic domain of calibration, a principle we call "geographic transferability". The GEDI footprint models are updatable as new calibration data become available. The first biomass map will be created using the first 12 months of data, and then monthly updates will be provided that include both new GEDI observations as well as any new calibration data in subsequent versions.

4.3.4.2. Level 4B. GEDI will produce a map showing estimates of mean AGBD at a resolution of 1 km or better for all latitudes covered by the ISS. Accurate gridded estimates of forest parameters such as AGBD are crucial for process models used to understand and predict interactions between dynamic forest ecosystems and the atmosphere (Hall et al., 2011). Importantly, mission requirements include corresponding estimates of variance for these estimates of the mean, necessitating a statistical framework and a formal process of inference. One of two approaches will be used for each 1 km grid cell, depending upon how many footprint-level (L4A) predictions of AGBD are available within the cell (Fig. 8).

For grid cells with few or no GEDI measurements, a process called generalized hierarchical model-based inference (GHMB) will be used (Saarela et al., 2016, 2018). In this process, all of the L4A AGBD predictions in a 10 × 10 km area containing the 1 km grid cell of interest are used to locally calibrate a Landsat-based biomass map for the cell, which becomes the basis for inferring 1 km cell-level mean biomass and its variance. GHMB variance estimators properly combine model uncertainty from both the L4A process and the Landsat-based model. Future work will explore combination of Landsat in this capacity with predictors from other wall-to-wall sensors, such as TanDEM-X.

Once footprint-level (L4A) AGBD estimates are available from at least two GEDI beam paths within a given cell, a simpler, single-stage estimation process becomes possible, requiring no use of ancillary wall-to-wall imagery. This process, called hybrid inference, frames GEDI's dense sample of biomass predictions in the same way a country's national forest inventory treats its sample plots – as a designed sample where every observation has an explicit probability of inclusion (Ståhl et al., 2016). At the same time, hybrid estimation also accounts for the fact that AGBD is modeled, not measured, from GEDI observables at each footprint (Patterson et al., 2019). Each beam path is conventionally considered a cluster sample (Healey et al., 2012; Ståhl et al., 2011), and two or more beam paths are needed to support hybrid inference because at least two clusters are required to generate a hybrid estimate of variance.

The L4B product for each grid cell will contain estimates for the AGBD mean and variance, along with information about the mode of inference (GHMB or hybrid) and the underlying observations: number of footprints, number of clusters, and parameters of the models used. L4A footprint-level predictions can support hybrid and GHMB inferences for areas larger than 1 km, or that are irregularly shaped or spatially discontinuous. Estimation for such areas would occur in parallel to the L4B gridded estimates, using all intersecting GEDI footprints.

5. The GEDI lidar instrument

The GEDI instrument is a self-contained, multi-beam laser altimeter. It is comprised of 3 lasers, an 80 cm beryllium telescope and secondary mirror, three star-trackers, a dedicated GPS, a pointing control system (PCS) as well as detectors, integrated flight electronics, heaters and cooling elements (Fig. 9).

The PCS provides cross-track pointing control over ±5.6° to reduce the significant measurement gaps that would otherwise result from the ISS orbit variations (Fig. 10) that occur because the ISS is not maintained in a repeating orbit (e.g. see Fig. 2).

A composite optical bench isolates the lasers, transmit optics, beam dithering units (BDUs, discussed below), receiver telescope assembly, IMU, and star trackers on a common bench to ensure on-orbit optical alignment stability (Fig. 11). Two lasers are used at 15 mJ/pulse and the third laser has a diffractive optical element that splits its output into two coverage beams of 4.5 mJ/pulse each. Each laser is fired through an external BDU that shifts the pulses 600 m across-track on alternating laser shots.

The telescope receiver system has an individual field of view (FOV) for each beam that fiber couples the return pulses to their respective detector channels, which use Silicon Avalanche Photodiode (Si:APD) detectors. The detector's analog signal is digitized at 1 Gsamp/sec with 12-bit Analog to Digital converters. The average daily data volume under nominal conditions is 85 Gbits per day.

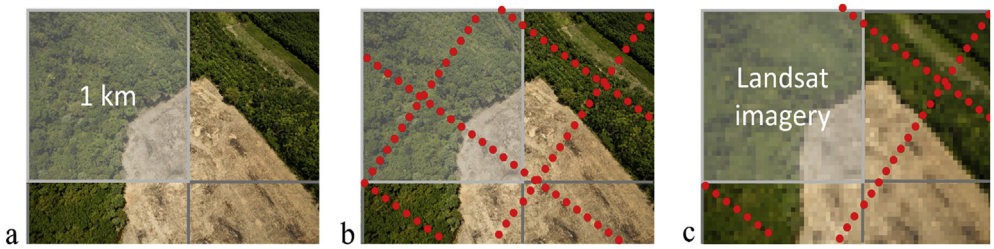

Fig. 8. Modes of inference applied to estimate mean AGBD for each 1 km grid cell (a). Hybrid inference will be applied in cells (b) with at least two beam passes (treated as sampling clusters), while generalized hierarchical model-based inference, based upon models calibrated outside the cell which use wall-to-wall imagery, will be employed in 1 km cells with few or no L4a footprints (c).

5.1. Lasers

GEDI implements the High Output Maximum Efficiency Resonator (HOMER), a Nd:YAG actively Q-switched laser with a unique oscillator-only layout employing Gaussian reflective optics and highly optimized laser slab design (Stysley et al., 2015; Coyle et al., 2015). The HOMER laser characteristics are as follows: pulse repetition rate of 242 Hz; pulse width of ~15 ns (full-width half-max); wavelength of 1064 nm; output power of 15 mJ; and single gaussian spatial mode. The HOMER design has completed lifetime testing in excess of 20 billion shots with negligible degradation.

5.2. Optics

The GEDI optics utilize a beam expander (BE) with an 18X magnification design producing a 56.1 μrad ($1/e^2$) beam divergence, that generates a 23 ± 2 m diameter footprint from the nominal 410 km altitude. Risley prisms attached to the output end of each BE are used for boresight alignment on the ground. A diffractive optical element (DOE) splits 1 of the 3 laser beams into 2 coverage beams.

Each laser has a BDU located prior to the BE. The BDU is implemented with switch crystals and a passive optical wedge to create two ground tracks from each beam. Dithering is achieved by first actively switching the HOMER laser beam between *s* and *p* polarization on alternating laser shots. The *s* and *p* polarized beams then enter a passive, birefringent optical wedge, sized and oriented such that the polarized beams separate, and then the wedge redirects the two separated beams back together onto the first optic of the beam expander.

The GEDI telescope is a light-weighted beryllium design, identical to the mirror used on ICESat-2 (indeed, the GEDI telescope was the ICESat-2 spare). Because ICESat-2 operates in the visible spectrum, the coatings on the GEDI telescope are not optimized for the near-IR, resulting in some small loss of reflectivity at 1 μm relative to the visible. Refractive aft-optics correct imaging over the entire FOV. Each beam has an instantaneous FOV (IFOV) that is fiber optically coupled to a detector. Each fiber produces an IFOV of 315 μrad in diameter, allowing for a 129-μrad boresight misalignment budget.

There is one detector assembly associated with each laser output beam for the coverage beam and the full power beams each have two independent detectors, 1 for each ground track. The combined inputs are passed through the bandpass filter and sent to the detector.

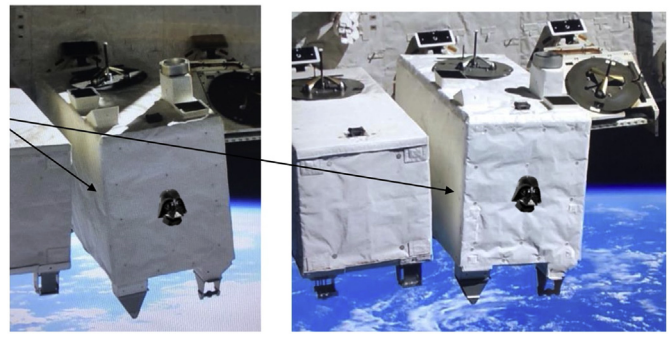

Fig. 10. GEDI pointing capability. Arrows show how the instrument may be pointed off-nadir to target specific locations and to fill-in gaps in coverage that occur from clouds and ISS orbital resonances.

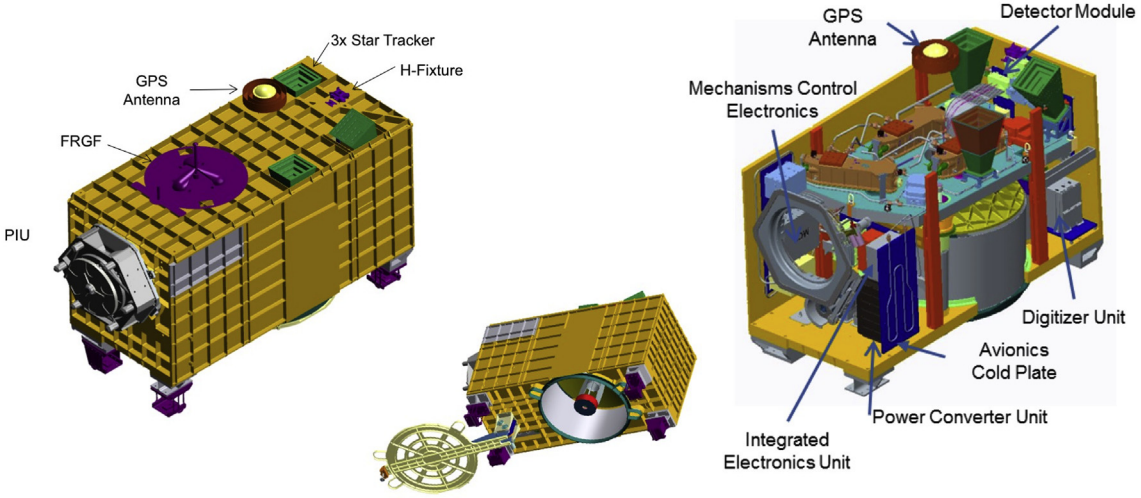

Fig. 9. The GEDI instrument. Abbreviations: PIU = payload interface unit. FRGF = grappling fixture. Middle diagram shows the instrument with the aperture door open.

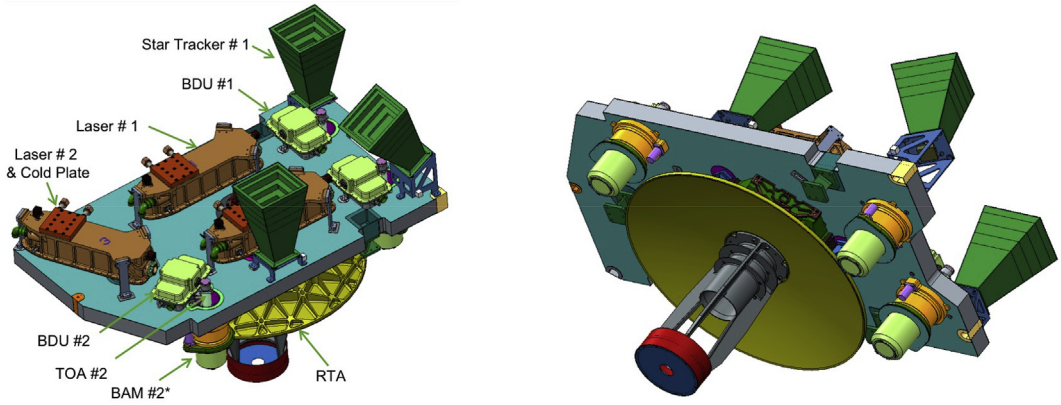

Fig. 11. The GEDI optical bench. Left figure shows rear of the bench, including the 3 laser transmitters, 3 beam dithering units (BDU), 3 star-trackers, 3 beam alignment mechanisms (BAM), and the receiver telescope assembly (RTA). Right figure shows the front with the 80 cm telescope and BAMS.

5.3. Instrument requirements on data quality

The GEDI instrument was designed to meet certain requirements on data quality that allow for the generation of data products sufficient to meet its L1 requirements. The key aspect of data quality is the vertical accuracy of the lidar-derived canopy height profiles of vegetation structure. To accurately capture the vertical structure of vegetation, SNR (i.e., sensitivity) is crucial because the instrument must be able to detect the weak signal from the ground in closed canopy conditions. Sufficient dynamic range of the receiver (i.e., ability to see weak and strong signals simultaneously) is required because a single waveform will contain a strong return from the overlying canopy and a signal from the ground below that can be 100 times weaker. Finally, sufficient vertical resolution is required to distinguish and determine the relative height of vegetation layers and the ground surface in each footprint. The GEDI design specifically addresses each of these factors to optimize measurement performance. The horizontal accuracy of the geolocated footprint is critical for data fusion and for the cal/val of the sensor data.

To achieve the sampling density and grid cell coverage required, GEDI requires sufficient SNR to fully perform even under non-ideal atmospheric attenuation conditions. This was evaluated using a detailed lidar link margin analysis (Hancock et al., 2019). The link margin is measured in units of dB and quantifies the difference between instrument sensitivity and the expected minimum return signal strength (i.e. how weak of ground signal can GEDI detect under various atmospheric, solar illumination, and canopy cover conditions). The link analysis was performed with the following parameters: orbital altitude: 410 km; laser output power: 15 mJ/4.5 mJ, atmospheric transmission: 0.6, surface reflectivity: 40%, receiver efficiency: 75%, as well as other parameters, for daytime and nighttime conditions. Solar background noise during the day in the near-IR decreases SNR. ICESat data was utilized to inform the model for atmospheric attenuation, surface roughness, surface reflectivity, and the like. Pre-launch analyses demonstrated that GEDI had sufficient capability and performance margin to meet its measurement requirements (Fig. 12).

The resolution of the range and height information derived from a single laser pulse is determined by the bandwidth of the lidar system, i.e., laser pulse width (15 ns FWHM), detector bandwidth (100 MHz), and the digitizer sampling rate and dynamic range (800 Msamp/s, 10 bits). For simple, unvegetated, relatively flat surfaces where the returned waveform is gaussian, the range precision is ~3 cm.

The GEDI <25 m footprint size requirement was chosen for four reasons: 1) based on the extensive experience with airborne waveform lidar; 2) large enough to capture the entire canopy of larger diameter trees; 3) large enough to ensure there will be enough gaps to allow detection of the underlying ground; and 4) small enough to limit the vertical mixing of vegetation and ground signals caused by surface slope.

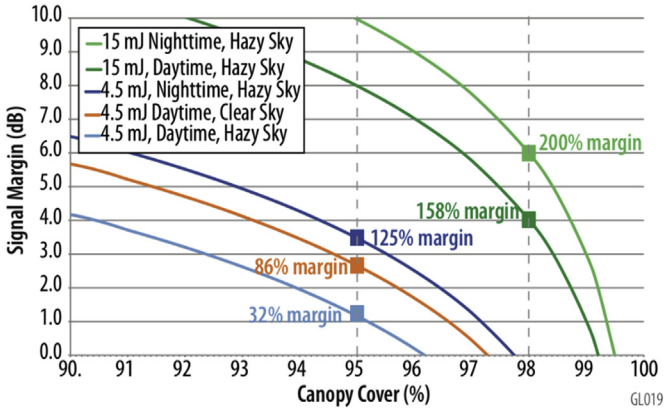

Fig. 12. GEDI pre-launch link margin results. Each line represents a different configuration of laser power and viewing conditions. A margin of 0 dB means that the instrument would detect the ground for a canopy cover given where the curve intersects the x-axis; for example, daytime coverage beam will detect the ground underneath canopy cover as great as 96%. GEDI was designed to penetrate 95% and 98% canopy cover with margin for the coverage and strong beams, respectively.

Studies using airborne data have shown that 1 m height accuracy can be achieved with 23 ± 2 m footprints over a wide variety of terrain and canopy conditions (Zolkos et al., 2013).

6. Mission and science operations

The GEDI Science and Mission Operations Center (SMOC) performs all mission operations, science data acquisition planning and optimization, computation and production of science data products, as well as delivery and archival of mission Level-0 data and delivery of all Level science data products to the NASA DAACs. The SMOC is located within NASA Goddard Space Flight Center's Science and Planetary Operations Control Center (SPOCC).

GEDI command and telemetry, including engineering and science data, are provided from the instrument to the ISS and downlinked through the Tracking Data Relay Satellite System (TDRSS) to the Payload Operations Integration Center (POIC) located in the Huntsville Operations and Support Center (HOSC) at Marshall Space Flight Center (MSFC). Command, control and telemetry (including science data) is provided through the POIC. Instrument command and control is provided as GEDI Absolute Time Sequence (ATS) and Relative Time Sequence (RTS) stored command loads. The SPOC also provides the stored load of the Reference Ground Tracks (RGT) that will be targeted via instrument active pointing. Instrument health and safety is monitored through

engineering telemetry and video as needed.

Science operations consist of the Science Planning System (SPS) and the Science Data Processing System (SDPS). The SPS uses ISS predicted orbits and attitude to compute the Science Activity Timeline (SAT) which includes instrument on/off and configuration setting for data acquisition land passes and calibration maneuvers. The SAT also includes commands for the Pointing Control System (PCS) as needed. As a companion to the SAT, the SPS computes the RGT locations for PCS pointing and data acquisition as a time series of Earth Centered Fixed (ECF) coordinates. The SAT and the RGT are created each day and provided to the mission operations to create 5-day instrument commands and RGT loads. The SPS computes all RGTs that can be acquired for each orbit and computes a nominal optimal RGT to be acquired in order to optimize coverage. The GEDI Science Team receives planning products each mission week to fine-tune and further optimize the RGTs for data acquisition. The SDPS generates the science data products and delivers the Level-0 and higher-Level data products to the NASA DAACs. The SDPS includes the computation of precise positioning of the GEDI instrument along with the post-processed instrument attitude and laser pointing solutions using the GEDI star tracker system data. Lastly, the SDPS includes the complex waveform processing for range computation and higher-level products. The positioning, pointing and ranging are then used to precisely geolocate the GEDI waveforms, while the waveform processing supports the higher-level data product production.

The ISS can present challenging environments for payloads during mission operations. For example, GEDI has experienced greater than expected blindings of its three star trackers. This is caused by glint off the structure of the ISS which prevents the star trackers from seeing stars. Pre-launch glint models did not accurately capture the true reflectance surfaces leading to longer than expected blinding durations during particular orbits. This in turn, hinders precision orbit determination and increases the time required to determine the geolocation of footprints. Additionally, operations by the ISS robotic arms and any payload they may be holding may block star tracker views, sometimes for days.

7. Calibration and validation

The GEDI calibration and validation (cal/val) program has been organized into pre-launch and post-launch activities. Prior to launch, cal/val activities were focused on the acquisition and processing of data with which to calibrate, test, and improve models and algorithms for application to GEDI science data products. Central to these activities are the GEDI Forest Structure and Biomass Database (FSBD) and the GEDI Performance Tool. The GEDI FSBD implements a common framework to standardize community contributed field and airborne lidar data across the entire geographic domain of GEDI. These data are used to simulate GEDI waveforms for algorithm calibration and are automatically collocated with on-orbit GEDI data for validation. The FSBD encompasses a broad range of tropical and temperate vegetation types globally (Fig. 13). Its development was a complex effort spanning many different organizations with airborne lidar observations acquired at 208 sites across six continents (1,532,699 trees from 5646 plots) incorporated to date. The GEDI Performance Tool links the FSBD with a laser link margin model (discussed above), GEDI waveform simulator (Hancock et al., 2019), ISS orbital simulations, and science data product algorithms to quantitatively assess the impact of changes to mission configuration and algorithm calibrations on sampling coverage and L1 mission requirements for biomass.

Post-launch cal/val activities target further validation of the science algorithms and assumptions, updating the calibration of any necessary algorithm parameters, and evaluation of the accuracy of science data products. Independent evaluation of footprint geolocation accuracy and waveform fidelity are important early steps post-launch. This is required to validate GEDI performance against design requirements, assess the repeatability of the GEDI Level 1 and 2 product variables, and verify their accuracy. The footprint level biomass pre-launch calibration strategy described in Section 4.3.4 is continuing into the post-launch phase of the mission as GEDI collaborative cal/val activities continue to expand. A critical assumption of the Level 4B product algorithm is that the Level 4A AGBD estimators are representative of the population to which they are applied. To ensure this assumption is not violated, geographic regions with a paucity of calibration data are a priority for evaluation and updates to post-launch calibration of the Level 4A product.

Validation of GEDI algorithms and products rely on comparisons using intra-mission and inter-mission datasets. Intra-mission comparisons use crossovers of GEDI ground tracks from intersecting ascending and descending orbits. Inter-mission comparisons use recent field and lidar acquisitions in the FSBD and a limited set of coincident ground and airborne campaigns. The first dedicated campaign was in May 2019, with flights by LVIS over tropical and temperate forest sites in Central America and the USA, respectively. Three categories of data acquisition were undertaken: (1) orbital underflights $>$ 1000 km for all GEDI beam configurations to underpin post-launch calibration and validation of Level 1 and 2 product algorithms; (2) east−west transects $>$ 1000 km to expand the range of GEDI laser periods and day/night conditions sampled; (3) large area (e.g., 100 $\times$ 30 km); and, (4) mapping boxes over established ground monitoring sites with historical LVIS data (e.g., La Selva Biological Station, Costa Rica). Collectively, these acquisitions expand the number of coincident observations from future GEDI orbits and existing ground plot networks and provide reference data on long-term (>10 years) accumulation and fluxes of terrestrial forest carbon stocks.

Collaboration with the science teams from other missions, both NASA and international, has been of significant benefit to the GEDI calibration and validation program. One key example is the AfriSAR campaign (Fatoyinbo et al., 2017), in which in situ and LVIS data coincident with polarimetric and interferometric SAR observations were collected over tropical forests in Gabon. Due to the challenging conditions for lidar measurements, this has been a core pre-launch algorithm cal/val site for GEDI and the prototyping of GEDI demonstrative products. Early on-orbit comparisons of GEDI returns with data collected during AfriSAR have confirmed its ability to measure the complex vertical canopy structure of these forests (Fig. 14).

8. Concluding remarks

The concept for a spaced-based lidar optimized for measuring ecosystem structure traces back now more than 20 years, to the first ESSP mission, the Vegetation Canopy Lidar, which was never completed. Since that time, numerous studies using airborne lidar, and the limited data from the ICESat mission, have underscored the crucial importance of obtaining three-dimensional information for ecosystems. Recognizing this importance, the international terrestrial ecology community has continued to advocate for an ecosystem lidar to meet increasingly urgent research needs in carbon cycle science, biodiversity studies, and other areas. GEDI represents a culmination of these long years of effort by this community.

Observations from GEDI should help us better understand the strengths and limitations of lidar as a technology deployed from space. In particular, we should be able to gain considerable insight into the efficacy of a set of instrument and mission design decisions that can be used to inform future missions, as follows.

First, there is the choice of lidar technology. There are currently two technologies in space at the moment, the near-IR waveform measurements from GEDI and the visible wavelength photon-counting measurements from ICESat-2. That we have both kinds of observations available for intercomparison simultaneously from space is a remarkable occurrence. Secondly, there is the consideration of laser power. Stronger lasers penetrate higher canopy cover, but this power must be balanced by issues of laser lifetime, beam quality, power consumption and repetition rate. There is also uncertainty about needed laser strength because we have incomplete information about the true magnitude of canopy cover above about 90% cover globally. GEDI observations should help clarify both the

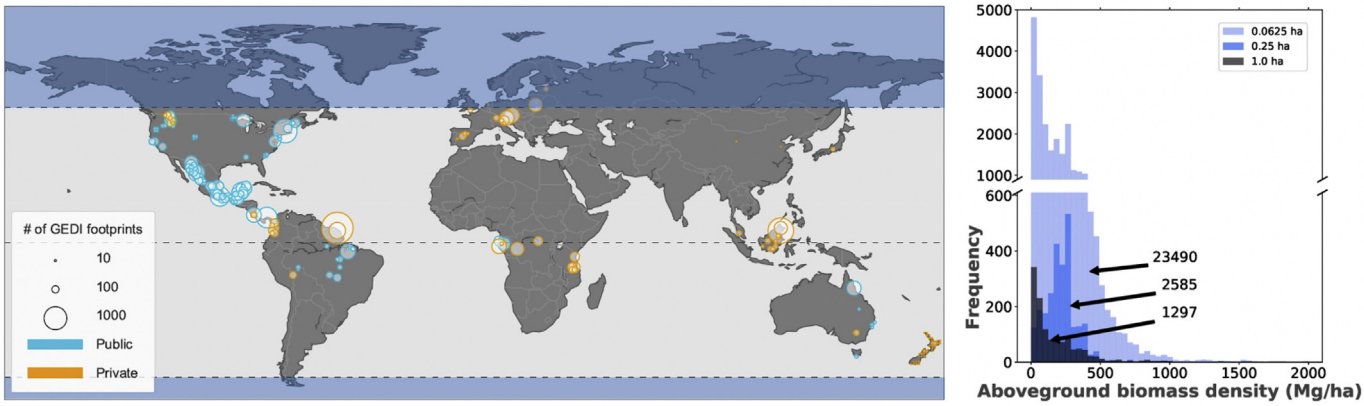

Fig. 13. Global distribution of sites with coincident field and ALS data in the GEDI Forest Structure Biomass Database (FSBD). Each site has its own characteristics in terms of number of field plots, public/private access and the number of simulated GEDI footprints (left panel). Original field plots were disparate in terms of plot measurement protocol, size, shape, and stem or subplot map availability so have undergone extensive QA/QC and standardization for inclusion in FSBD. This enables consistent use of all available data at multiple spatial resolutions (right panel).

global cover distribution at these high levels, as well as the ability of strong and less-strong lasers to penetrate these under a variety of solar illumination and atmospheric conditions. There is further the issue of footprint size and its relationship to canopy diameter and topography. The GEDI footprint size was chosen based on our desire to limit the effects of topographic slope for canopy measurements, while also being large enough to capture the entire canopy of large trees and provide suitable measurements for biomass estimation. GEDI should illuminate both the impact of footprint size as well as the efficacy of a pre-calibration strategy that avoids the requirement of stringent geolocation to develop biomass calibration equations, while also providing information on the quantity and quality of the needed ground data. Lastly, we should develop a much better realization of the value of sampling over large areas across-track and non-contiguously along track

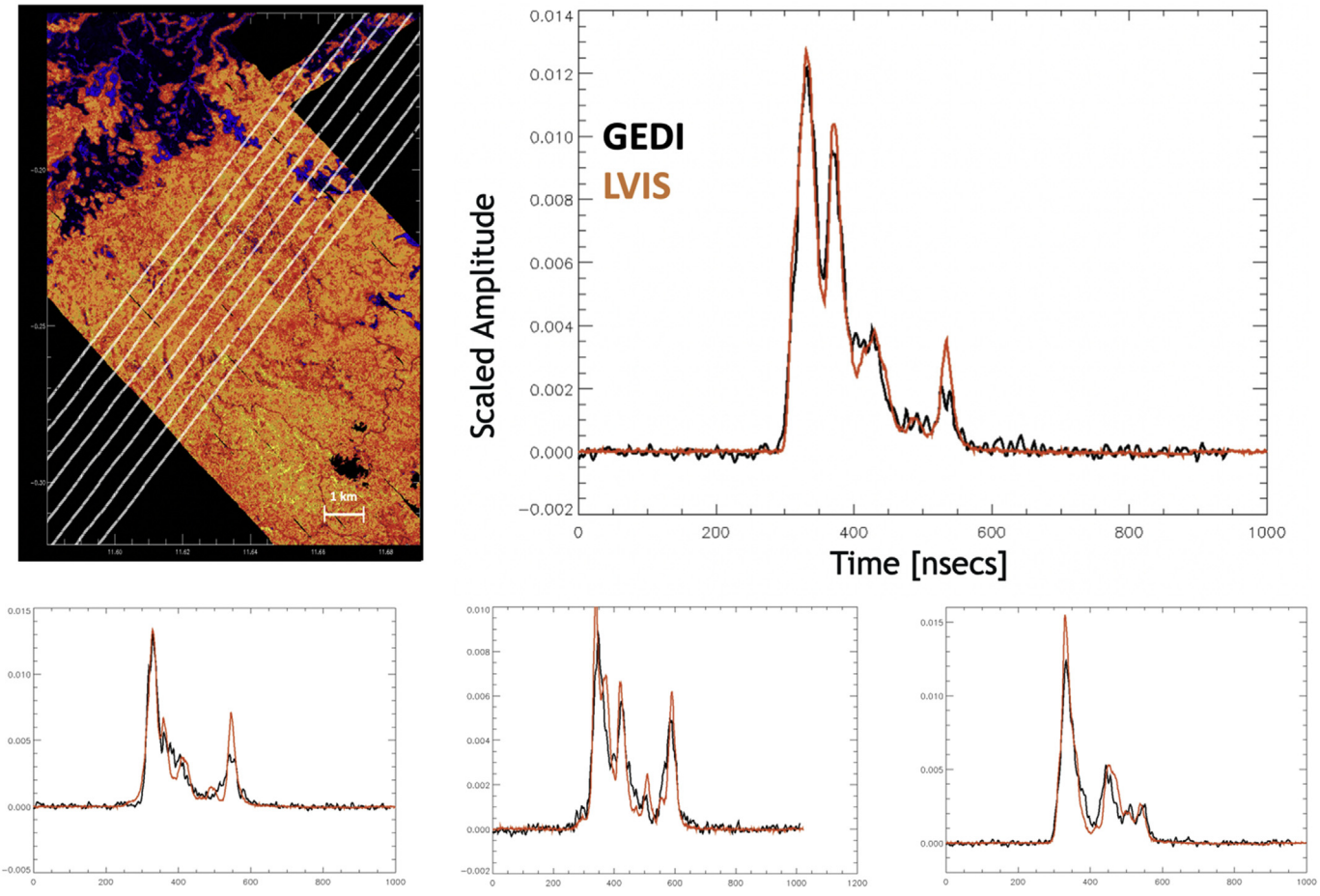

Fig. 14. Comparison of GEDI on-orbit waveforms with airborne waveforms from LVIS over the AfriSAR site in Gabon. Map on left shows the 8 tracks of GEDI data over the LVIS coverage. Waveforms show GEDI strong beam returns (in black) and LVIS returns (red). (For interpretation of the references to colour in this figure legend, the reader is referred to the Web version of this article.)

(the strategy employed by GEDI) as opposed to concentrating observations to better characterize local areas.

While the GEDI mission may be short-lived, it promises to revolutionize our understanding of the role of ecosystem structure. Furthermore, the recent availability of data from other sensors contemporaneous with GEDI on the ISS, such as ECOSTRESS, OCO-3, and HISUI (Stavros et al., 2017) is a watershed moment in ecosystem science where the simultaneous observation of structure, function and composition is now a reality. Our hope is that GEDI sets the stage for more advanced lidar concepts from space because GEDI is not the last lidar mission, it is simply the next one.

Acknowledgements

This work is funded by NASA contract #NNL 15AA03C to the University of Maryland for the development and execution of the GEDI mission (Dubayah, Principal Investigator). We thank the NASA Terrestrial Ecology program for continued support of the GEDI mission. The University of Maryland has also provided independent financial support of the GEDI mission. We gratefully acknowledge the efforts of David Minor, Chenguang Huang, Jamis Bruenig, Patrick Burns, and Seung Kuk Lee towards the implementation and execution of GEDI. The German Aerospace Center (DLR) is formal collaborator of the GEDI mission and we thank them for their support of DLR scientists Drs. Kostas Papathanassiou and Matteo Pardini towards the implementation of fusion methods for GEDI and TanDEM-X.

The paper was conceived and written by RD with other contributions as follows. BB and SG are Deputy Principal Investigators and LF, MHa, SHe, MH, GH, JK and SL are Co-Investigators of GEDI. All contributed writing and editing to various sections of the paper. JA provided inputs to the cal/val section, and along with HT, provided inputs on L2A and L2B algorithms and graphics, assisted by CS; LD provided inputs to the L4A section. PP provided inputs to the L4B section; SHa developed the GEDI simulator and provided other inputs; PJ and WQ provided inputs to Demonstrative products. SM provided substantial editorial support of this paper, as well as supporting data analysis

References

Abdalati, W., Zwally, H.J., Bindschadler, R., Csatho, B., Farrell, S.L., Fricker, H.A., Harding, D., Kwok, R., Lefsky, M., Markus, T., Marshak, A., Neumann, T., Palm, S., Schutz, B., Smith, B., Spinhirne, J., Webb, C., 2010. The ICESat-2 laser altimetry mission. Proc. IEEE. https://doi.org/10.1109/JPROC.2009.2034765.

Armston, J., Disney, M., Lewis, P., Scarth, P., Phinn, S., Lucas, R., Bunting, P., Goodwin, N., 2013. Direct retrieval of canopy gap probability using airborne waveform lidar. Remote Sens. Environ. 134, 24–38.

Baccini, A., Goetz, S.J.J., Walker, W.S.S., Laporte, N.T.T., Sun, M., Sulla-Menashe, D., Hackler, J., Beck, P.S.A.S.A., Dubayah, R., Friedl, M.A.A., Samanta, S., Houghton, R.A.A., 2012. Estimated carbon dioxide emissions from tropical deforestation improved by carbon-density maps. Nat. Clim. Change 2. https://doi.org/10.1038/nclimate1354.

Bergen, K.M., Goetz, S.J., Dubayah, R.O., Henebry, G.M., Hunsaker, C.T., Imhoff, M.L., Nelson, R.F., Parker, G.G., Radeloff, V.C., 2009. Remote sensing of vegetation 3-D structure for biodiversity and habitat: review and implications for lidar and radar spaceborne missions. J. Geophys. Res. 114, 13.

Blair, J.B., Rabine, D.L., Hofton, M.A., 1999. The Laser Vegetation Imaging Sensor: a medium-altitude, digitisation-only, airborne laser altimeter for mapping vegetation and topography. Isprs J. Photogramm. Remote Sens. 54, 115–122.

Brancalion, P.H.S., Niamir, A., Broadbent, E., Crouzeilles, R., Barros, F.S.M., Almeyda Zambrano, A.M., Baccini, A., Aronson, J., Goetz, S., Leighton Reid, J., Strassburg, B.B.N., Wilson, S., Chazdon, R.L., 2019. Global restoration opportunities in tropical rainforest landscapes. Sci. Adv. https://doi.org/10.1126/sciadv.aav3223.

Burns, P., Clark, M., Hofton, M., Jantz, P., Leland, D., Dubayah, R., Goetz, S., 2020. Incorporating canopy structure from simulated GEDI lidar into bird species distribution models. Enivron. Res. Lett. Submitted for publication.

Coyle, D.B., Stysley, P.R., Poulios, D., Clarke, G.B., Kay, R.B., 2015. Lidar Remote Sens. Environ. Monit. XV.

De Vos, J.M., Joppa, L.N., Gittleman, J.L., Stephens, P.R., Pimm, S.L., 2015. Estimating the normal background rate of species extinction. Conserv. Biol. https://doi.org/10.1111/cobi.12380.

Drake, J.B., Dubayah, R.O., Knox, R.G., Clark, D.B., Blair, J.B., 2002. Sensitivity of large-footprint lidar to canopy structure and biomass in a neotropical rainforest. Remote Sens. Environ. 81 https://doi.org/10.1016/S0034-4257(02)00013-5.

Dubayah, R., Sheldon, S., Clark, D., Hofton, M., Blair, J.B., Hurtt, G., Chazdon, R., 2010. Estimation of tropical forest height and biomass dynamics using lidar remote sensing at La Selva, Costa Rica. J. Geophys. Res. 115 (G00E09) https://doi.org/10.1029/2009JG000933.

Fatoyinbo, T., Pinto, N., Hofton, M., Simard, M., Blair, J.B., Saatchi, S.S., Lou, Y., Dubayah, R., Hensley, S., Armston, J.D., Duncanson, L., Lavalle, M., 2017. In: IEEE International Geoscience and Remote Sensing Symposium (IGARSS).

Garvin, J., Bufton, J., Blair, J., Harding, D., Luthcke, S., Frawley, J., Rowlands, D., 1998. Observations of the earth's topography from the Shuttle Laser Altimeter (SLA): laser-pulse echo-recovery measurements of terrestrial surfaces. Phys. Chem. Earth. https://doi.org/10.1016/S0079-1946(98)00145-1.

Hall, F.G., Bergen, K., Blair, J.B., Dubayah, R., Houghton, R., Hurtt, G., Kellndorfer, J., Lefsky, M., Ranson, J., Saatchi, S., Shugart, H.H., Wickland, D., 2011. Characterizing 3D vegetation structure from space: mission requirements. Remote Sens. Environ. 115, 2753–2775.

Hancock, S., Armston, J., Hofton, M., Sun, X., Tang, H., Duncanson, L.I., Kellner, J.R., Dubayah, R., 2019. The GEDI simulator: a large-footprint waveform lidar simulator for calibration and validation of spaceborne missions. Earth Sp. Sci. 6, 294–310.

Hansen, M.C., Potapov, P.V., Moore, R., Hancher, M., Turubanova, S.A., Tyukavina, A., Thau, D., V Stehman, S., Goetz, S.J., Loveland, T.R., Kommareddy, A., Egorov, A., Chini, L., Justice, C.O., Townshend, J.R.G., 2013. High-resolution global maps of 21st-century forest cover change. Science (80–.). https://doi.org/10.1126/science.1244693.

Hansen, M.C., Stehman, S.V., Potapov, P.V., 2010. Quantification of global gross forest cover loss. Proc. Natl. Acad. Sci. https://doi.org/10.1073/pnas.0912668107.

Harris, N.L., Brown, S., Hagen, S.C., Saatchi, S.S., Petrova, S., Salas, W., Hansen, M.C., Potapov, P.V., Lotsch, A., 2012. Baseline map of carbon emissions from deforestation in tropical regions. Science (80-.). https://doi.org/10.1126/science.1217962.

Healey, S.P., Patterson, P.L., Saatchi, S., Lefsky, M.A., Lister, A.J., Freeman, E.A., 2012. A sample design for globally consistent biomass estimation using lidar data from the Geoscience Laser Altimeter System (GLAS). Carbon Bal. Manag. https://doi.org/10.1186/1750-0680-7-10.

Hofton, M.A., Minster, J.B., Blair, J.B., 2000. Decomposition of laser altimeter waveforms. IEEE Trans. Geosci. Rem. Sens. https://doi.org/10.1109/36.851780.

Houghton, R.A., 2003. Why are estimates of the terrestrial carbon balance so different? Global Change Biol. https://doi.org/10.1046/j.1365-2486.2003.00620.x.

Houghton, R.A., 2013. The emissions of carbon from deforestation and degradation in the tropics: past trends and future potential. Carbon Manag. https://doi.org/10.4155/cmt.13.41.

Houghton, R.A., Greenglass, N., Baccini, A., Cattaneo, A., Goetz, S., Kellndorfer, J., Laporte, N., Walker, W., 2010. The role of science in reducing emissions from deforestation and forest degradation (REDD). Carbon Manag. 1, 253–259.

Houghton, R.A., Hall, F., Goetz, S.J., 2009. Importance of biomass in the global carbon cycle. J. Geophys. Res. Biogeosci. https://doi.org/10.1029/2009JG000935.

Hurtt, G.C., Dubayah, R., Drake, J., Moorcroft, P.R., Pacala, S.W., Blair, J.B., Fearon, M.G., 2004. Beyond potential vegetation: combining lidar data and a height-structured model for carbon studies. Ecol. Appl. https://doi.org/10.1890/02-5317.

Hurtt, G.C., Fisk, J., Thomas, R.Q., Dubayah, R., Moorcroft, P.R., Shugart, H.H., 2010. Linking models and data on vegetation structure. J. Geophys. Res. Biogeosci. https://doi.org/10.1029/2009jg000937.

Hurtt, G.C., Moorcroft, P.R., Pacala, S.W., Levin, S.A., 1998. Terrestrial models and global change: challenges for the future. Global Change Biol. https://doi.org/10.1046/j.1365-2486.1998.00203.x.

Hurtt, G.C.C., Thomas, R.Q.Q., Fisk, J.P.P., Dubayah, R.O.O., Sheldon, S.L.L., 2016. The impact of fine-scale disturbances on the predictability of vegetation dynamics and carbon flux. PloS One 11. https://doi.org/10.1371/journal.pone.0152883.

Hurtt, G., Zhao, M., Sahajpal, R., Armstrong, A., Birdsey, R., Campbell, E., Dolan, K., Dubayah, R., Fisk, J.P., Flanagan, S., Huang, C., Huang, W., Johnson, K., Lamb, R., Ma, L., Marks, R., O'Leary, D., O'Neil-Dunne, J., Swatantran, A., Tang, H., 2019. Beyond MRV: high-resolution forest carbon modeling for climate mitigation planning over Maryland, USA. Environ. Res. Lett. https://doi.org/10.1088/1748-9326/ab0bbe.

Huston, M.A., 1994. Biological Diversity: the Coexistence of Species. Cambridge Univ. Press.

IPCC, Solomon, S., Qin, D., Manning, M., Chen, Z., Marquis, M., Averyt, K.B., Tignor, M., Miller, H.L., 2007. Cambridge University Press, Cambridge, United Kingdom and New York, NY, USA, p. 996.

IUCN, International Union for the Conservation of Nature Red List, 2019. available at: http://www.iucnredlist.org.

Jantz, P., Goetz, S., Laporte, N., 2014. Carbon stock corridors to mitigate climate change and promote biodiversity in the tropics. Nat. Clim. Change 4, 138–142.

Knapp, N., Fischer, R., Huth, A., 2018. Linking lidar and forest modeling to assess biomass estimation across scales and disturbance states. Remote Sens. Environ. https://doi.org/10.1016/j.rse.2017.11.018.

Krieger, G., Moreira, A., Fiedler, H., Hajnsek, I., Werner, M., Younis, M., Zink, M., 2007. In: IEEE Transactions on Geoscience and Remote Sensing.

Le Toan, T., Quegan, S., Davidson, M.W.J., Balzter, H., Paillou, P., Papathanassiou, K., Plummer, S., Rocca, F., Saatchi, S., Shugart, H., Ulander, L., 2011. The BIOMASS mission: mapping global forest biomass to better understand the terrestrial carbon cycle. Remote Sens. Environ. 115, 2850–2860.

Luthcke, S.B., Rowlands, D.D., McCarthy, J.J., Pavlis, D.E., Stoneking, E., 2000. Spaceborne laser-altimeter-pointing bias calibration from range residual analysis. J. Spacecraft Rockets 37, 374–384.

Luthcke, S.B., Rowlands, D.D., Williams, T.A., Sirota, M., 2005. Reduction of ICESat systematic geolocation errors and the impact on ice sheet elevation change detection. Geophys. Res. Lett. https://doi.org/10.1029/2005GL023689.

MacArthur, R.H., MacArthur, J.W., 1961. On Bird Species Diversity. On Bird Species Diversity. Ecology. https://doi.org/10.2307/1932254.
Mace, G., Masundire, H., Baillie, J., 2005. In: Hassan, R.M., Scholes, R.J., Ash, N. (Eds.), Ecosystems and Human Well-Being: Current State and Trends: Findings of the Condition of Trends Working Group. The Millennium Ecosystem Assessment Series, V1. Island Press.
Mitchard, E.T.A., Saatchi, S.S., Baccini, A., Asner, G.P., Goetz, S.J., Harris, N.L., Brown, S., 2013. Uncertainty in the spatial distribution of tropical forest biomass: a comparison of pan-tropical maps. Carbon Bal. Manag. https://doi.org/10.1186/1750-0680-8-10.
Moorcroft, P.R., Hurtt, G.C., Pacala, S.W., 2001. A method for scaling vegetation dynamics: the ecosystem demography model. Ecol. Monogr. https://doi.org/10.1890/0012-9615(2001)071[0557:AMFSVD]2.0.CO;2.
National Research Council, 2007. Earth Science and Applications from Space: National Imperatives for the Next Decade and beyond. The National Academies Press, Washington, DC.
Ni-Meister, W., Jupp, D.L.B., Dubayah, R., 2001. Modeling lidar waveforms in heterogeneous and discrete canopies. IEEE Trans. Geosci. Rem. Sens. 39, 1943–1958.
Pan, Y., Birdsey, R.A., Fang, J., Houghton, R., Kauppi, P.E., Kurz, W.A., Phillips, O.L., Shvidenko, A., Lewis, S.L., Canadell, J.G., Ciais, P., Jackson, R.B., Pacala, S.W., McGuire, A.D., Piao, S., Rautiainen, A., Sitch, S., Hayes, D., 2011. A large and persistent carbon sink in the world's forests. Science (80-.). https://doi.org/10.1126/science.1201609.
Patterson, P.L., Healey, S.P., Ståhl, G., Saarela, S., Holm, S., Andersen, H.-E., Dubayah, R., Duncanson, L., Hancock, S., Armston, J., Kellner, J.R., Cohen, W.B., Yang, Z., 2019. Statistical properties of hybrid estimators proposed for GEDI – NASA's Global Ecosystem Dynamics Investigation. Environ. Res. Lett. 14, 65007.
Pereira, H.M., Ferrier, S., Walters, M., Geller, G.N., Jongman, R.H.G., Scholes, R.J., Bruford, M.W., Brummitt, N., Butchart, S.H.M., Cardoso, A.C., Coops, N.C., Dulloo, E., Faith, D.P., Freyhof, J., Gregory, R.D., Heip, C., Höft, R., Hurtt, G., Jetz, W., Karp, D.S., McGeoch, M.A., Obura, D., Onoda, Y., Pettorelli, N., Reyers, B., Sayre, R., Scharlemann, J.P.W., Stuart, S.N., Turak, E., Walpole, M., Wegmann, M., 2013. Essential biodiversity variables. Science (80-.) 339, 277–278.
Petit, G., Luzum, B. (Eds.), 2010. IERS Conventions (2010), (IERS Technical Note ; 36) Frankfurt am Main: Verlag des Bundesamts für Kartographie und Geodäsie, 179 pp., ISBN 3-89888-989-6.
Pimm, S.L., Jenkins, C.N., Abell, R., Brooks, T.M., Gittleman, J.L., Joppa, L.N., Raven, P.H., Roberts, C.M., Sexton, J.O., 2014. The biodiversity of species and their rates of extinction, distribution, and protection. Science (80-.) 344. https://doi.org/10.1126/science.1246752.
Pimm, S.L., Raven, P., 2000. Extinction by numbers. Nature. https://doi.org/10.1038/35002708.
Qi, W., Saarela, S., Armston, J., Stahl, G., Dubayah, R., 2019. Forest biomass estimation over three distinct forest types using TanDEM-X InSAR data and simulated GEDI lidar data. Remote Sens. Environ. 232 https://doi.org/10.1016/j.rse.2019.111283.
Quéré, C., Andrew, R., Friedlingstein, P., Sitch, S., Hauck, J., Pongratz, J., Pickers, P., Ivar Korsbakken, J., Peters, G., Canadell, J., Arneth, A., Arora, V., Barbero, L., Bastos, A., Bopp, L., Ciais, P., Chini, L., Ciais, P., Doney, S., Gkritzalis, T., Goll, D., Harris, I., Haverd, V., Hoffman, F., Hoppema, M., Houghton, R., Hurtt, G., Ilyina, T., Jain, A., Johannessen, T., Jones, C., Kato, E., Keeling, R., Klein Goldewijk, K., Landschützer, P., Lefèvre, N., Lienert, S., Liu, Z., Lombardozzi, D., Metzl, N., Munro, D., Nabel, J., Nakaoka, S.I., Neill, C., Olsen, A., Ono, T., Patra, P., Peregon, A., Peters, W., Peylin, P., Pfeil, B., Pierrot, D., Poulter, B., Rehder, G., Resplandy, L., Robertson, E., Rocher, M., Rödenbeck, C., Schuster, U., Skjelvan, I., Séférian, R., Skjelvan, I., Steinhoff, T., Sutton, A., Tans, P., Tian, H., Tilbrook, B., Tubiello, F., Van Der Laan-Luijkx, I., Van Der Werf, G., Viovy, N., Walker, A., Wiltshire, A., Wright, R., Zaehle, S., Zheng, B., 2018. Global carbon budget 2018. Earth Syst. Sci. Data. https://doi.org/10.5194/essd-10-2141-2018.
Rosen, P.A., Hensley, S., Shaffer, S., Veilleux, L., Chakraborty, M., Misra, T., Bhan, R., Raju Sagi, V., Satish, R., 2015. In: IEEE National Radar Conference - Proceedings.
Saarela, S., Holm, S., Grafström, A., Schnell, S., Næsset, E., Gregoire, T.G., Nelson, R.F., Ståhl, G., 2016. Hierarchical model-based inference for forest inventory utilizing three sources of information. Ann. For. Sci. https://doi.org/10.1007/s13595-016-0590-1.
Saarela, S., Holm, S., Healey, S.P., Andersen, H.E., Petersson, H., Prentius, W., Patterson, P.L., Næsset, E., Gregoire, T.G., Ståhl, G., 2018. Generalized hierarchical model-based estimation for aboveground biomass assessment using GEDI and landsat data. Rem. Sens. https://doi.org/10.3390/rs10111832.
Saatchi, S.S., Harris, N.L., Brown, S., Lefsky, M., Mitchard, E.T.A., Salas, W., Zutta, B.R., Buermann, W., Lewis, S.L., Hagen, S., Petrova, S., White, L., Silman, M., Morel, A., 2011. Benchmark map of forest carbon stocks in tropical regions across three continents. Proc. Natl. Acad. Sci. https://doi.org/10.1073/pnas.1019576108.
Schnell, J.K., Harris, G.M., Pimm, S.L., Russell, G.J., 2013. Quantitative analysis of forest fragmentation in the Atlantic forest reveals more threatened bird species than the current red list. PloS One. https://doi.org/10.1371/journal.pone.0065357.
Schutz, B.E., Zwally, H.J., Shuman, C.A., Hancock, D., DiMarzio, J.P., 2005. Overview of the ICESat mission. Geophys. Res. Lett. https://doi.org/10.1029/2005GL024009.
Secretariat of the convention on biological diversity. Glob. Biodivers. Outlook 3, 2010.
Ståhl, G., Holm, S., Gregoire, T.G., Gobakken, T., Næsset, E., Nelson, R., 2011. Model-based inference for biomass estimation in a LiDAR sample survey in Hedmark County, Norway. Can. J. For. Res. 41, 96–107.
Ståhl, G., Saarela, S., Schnell, S., Holm, S., Breidenbach, J., Healey, S.P., Patterson, P.L., Magnussen, S., Næsset, E., McRoberts, R.E., Gregoire, T.G., 2016. Use of models in large-area forest surveys: comparing model-assisted, model-based and hybrid estimation. For. Ecosyst. https://doi.org/10.1186/s40663-016-0064-9.
Stavros, E.N., Schimel, D., Pavlick, R., Serbin, S., Swann, A., Duncanson, L., Fisher, J., Fassnacht, F., Ustin, S., Dubayah, R., Schweiger, A., Wennberg, P., et al., 2017. ISS observations offer insights into plant function. Nat Ecol Evol 1, 194. https://doi.org/10.1038/s41559-017-0194.
Stysley, P.R., Coyle, D.B., Kay, R.B., Frederickson, R., Poulios, D., Cory, K., Clarke, G., 2015. Long term performance of the high output Maximum efficiency resonator (HOMER) laser for NASA's global ecosystem dynamics investigation (GEDI) lidar. Optic Laser. Technol. https://doi.org/10.1016/j.optlastec.2014.11.001.
Tang, H., Dubayah, R., Swatantran, A., Hofton, M., Sheldon, S., Clark, D.B., Blair, B., 2012. Retrieval of vertical LAI profiles over tropical rain forests using waveform lidar at La Selva, Costa Rica. Remote Sens. Environ. 124, 242–250.
Thomas, R.Q., Hurtt, G.C., Dubayah, R., Schilz, M.H., 2008. Using lidar data and a height-structured ecosystem model to estimate forest carbon stocks and fluxes over mountainous terrain. Can. J. Rem. Sens. https://doi.org/10.5589/m08-036.
Torres, R., Snoeij, P., Geudtner, D., Bibby, D., Davidson, M., Attema, E., Potin, P., Rommen, B.Ö., Floury, N., Brown, M., Traver, I.N., Deghaye, P., Duesmann, B., Rosich, B., Miranda, N., Bruno, C., L'Abbate, M., Croci, R., Pietropaolo, A., Huchler, M., Rostan, F., 2012. GMES Sentinel-1 mission. Remote Sens. Environ. https://doi.org/10.1016/j.rse.2011.05.028.
Turner, W., Spector, S., Gardiner, N., Fladeland, M., Sterling, E., Steininger, M., 2003. Remote sensing for biodiversity science and conservation. Trends Ecol. Evol. 18, 306–314.
Tyukavina, A., Baccini, A., Hansen, M.C., V Potapov, P., V Stehman, S., Houghton, R.A., Krylov, A.M., Turubanova, S., Goetz, S.J., 2015. Aboveground carbon loss in natural and managed tropical forests from 2000 to 2012. Environ. Res. Lett. https://doi.org/10.1088/1748-9326/10/7/074002.
Whittaker, R.J., Willis, K.J., Field, R., 2001. Scale and species richness: towards a general, hierarchical theory of species diversity. J. Biogeogr. https://doi.org/10.1046/j.1365-2699.2001.00563.x.
Zolkos, S.G., Goetz, S.J., Dubayah, R., 2013. A meta-analysis of terrestrial aboveground biomass estimation using lidar remote sensing. Remote Sens. Environ. 128 https://doi.org/10.1016/j.rse.2012.10.017.